molecule. In fact, the value of the smallest positive perpendicular eigenvalue, λ_2, actually increases.

Ab initio SCF calculations on the isolobal complex $[(\eta^5\text{-}C_5H_5)Co(\mu\text{-}NO)]_2$, which experimentally possesses a much smaller Co–Co separation of 2.372 (1) Å,[27] yield a (3,-1) bond critical point between the Co atoms.[28] In order to observe how the topology of the density of $Co_2(CO)_8$ changes with a shorter Co–Co separation, the SCF calculation was performed with a Co–Co separation of 2.37 Å. The density of this geometry of $Co_2(CO)_8$ now possesses a (3,-1) bond critical point between the Co atoms. This critical point is located 0.02 Å "below" the Co–Co axis opposite the bridging carbonyls. The values of the perpendicular eigenvalues for this critical point are quite small at -0.0267 and -0.00833. This behavior is an indication of the flat nature of the charge density inside the $Co_2(\mu\text{-}C)_2$ ring. The density need not change much to alter the nature of the critical point between the cobalt atoms.

Conclusions

According to the topology of the charge density alone, there is no direct Co–Co bond in $Co_2(CO)_8$. All of the formal bonds between the two cobalt atoms occur through the bridging carbonyls. Therefore, the accumulations observed in the bent-bond regions of both the standard deformation density and the fragment deformation density maps are not sufficient to produce enough concentration of density between the cobalt atoms to form a bond.

However in the "nonbonded" fragment deformation density, the d_{yz} orbitals in each $Co(CO)_3$ fragment in the promolecule are already doubly occupied. So the accumulation in the Co–Co "bent-bond" region is most likely due to constructive interference between the two cobalt d_{yz} fragment orbitals. If one compares the standard deformation densities of the bridged and unbridged isomers, it could be suggested that if the unbridged isomer has a single Co–Co bond, then the bridged isomer has a bond order of $^1/_3$. However, this weak Co–Co interaction is not sufficient to alter the topology of the charge density enough to produce a (3,-1) bond critical point between the cobalt atoms.

Because the density and its derivatives are 1-electron properties, one would expect our results to be relatively stable with respect to the changes in the wave function introduced by electron correlation. We have carried out some preliminary configuration interaction calculations on $Co_2(CO)_8$[29] and more extensive calculations on the isolobal $Cp_2Co_2(NO)_2$.[28] Basically, in $Co_2(CO)_8$ the correlated wave function is strongly dominated by the single-determinant HFR configuration. In these situations previous results have shown that the density and its derivatives are qualitatively left unchanged by the addition of electron correlation.[30]

Registry No. $Co_2(CO)_8$, 10210-68-1.

(27) Bernal, I.; Korp, J. D.; Reisner, G. M.; Hermann, W. A. *J. Organomet. Chem.* **1977**, *139*, 321.
(28) Low, A. A.; Hall, M. B. To be submitted for publication in *Inorg. Chem.*
(29) Kunze, K. L.; Hall, M. B. Unpublished results.
(30) Gatti, C.; MacDougall, P. J.; Bader, R. F. W. *J. Chem. Phys.* **1988**, *88*, 3792.

Contribution from the Department of Chemistry and Materials Science Center, Cornell University, Ithaca, New York 14853, and Departament de Quimica Inorgânica, Universitat de Barcelona, Diagonal 647, Barcelona 08028, Spain

Electronic Structure of a $[Tc_2(\mu\text{-}O)_3Cp]_n$ Polymer with a Very Short Metal–Metal Bond

A. W. Edith Chan,[†] Roald Hoffmann,*[,†] and Santiago Alvarez[‡]

Received May 18, 1990

This recently synthesized polymer (with C_5Me_5) has a very short Tc–Tc distance of 1.867 Å. Its electronic structure is discussed by using molecular models and band calculations. The net bonding in a model $CpTcO_3TcCp^-$ is best described qualitatively as $\sigma^2(\pi\delta)^4\delta^*$, i.e. a net bond of approximate order 2.5. The details of the polymer's electronic structure are consistent with this. While bonding in multiply bridged dimers or polymers is never easy to sort out, we think the short Tc–Tc bond is consonant with a multiple metal–metal bond superimposed on an already short Tc–Tc contact enforced by the three bridging oxygens.

Recently, a polymeric compound with an extremely short technetium–technetium distance, $[Tc_2(\mu\text{-}O)_3(C_5Me_5)]_n$, was reported.[1] The unusually short metal–metal bond (1.867 Å) and the 3.5+ formal oxidation state of each Tc clearly suggest a multiple bond between the two metals. Around 20 Tc dimers have been synthesized in the past 20 years.[2] The Tc–Tc distances in these usually range from 2.05 to 3.14 Å. Many of these dimers are supported by bridging ligands, and only a few are held together by a direct metal–metal bond. Typical of these is quadruply bonded $Tc_2Cl_8^{2-}$, which has a Tc–Tc bond length of 2.14 Å.[3] The shortest previously reported Tc–Tc separation is 2.05 Å, in $Tc_2Cl_6^{2-}$.[4] So the much shorter bond in the Kanellakopulos and Ziegler polymer is truly striking. While supershort Cr–Cr bonds exist, and are quite well understood, there is no obvious rationale for the unusually short Tc–Tc distance in this polymer. Our study explores the bonding in this molecule, probing the nature of the metal–metal bond in it, and the role of the bridging oxygens. It should be noted that the Tc_2O_3Cp structure has been questioned;[5] there is a real scientific argument brewing. Whichever way it is resolved, i.e. whether the structure of the polymer is correct or not, it is interesting to think about such a chain and its bonding.

Structure **1** shows a view of the polymer. In molecules where a metal–metal bond is bridged by other ligands, it has never been

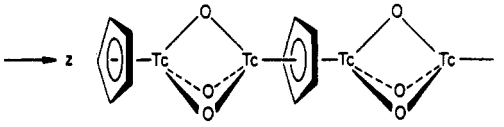

1

easy to sort out direct metal–metal bonding from bridging. One

[†] Cornell University.
[‡] Universitat de Barcelona.

(1) Kanellakopulos, B.; Nuber, B.; Raptis, K.; Ziegler, M. L. *Angew. Chem.* **1989**, *101*, 1055; *Angew. Chem., Int. Ed. Engl.* **1989**, *28*, 1055.
(2) (a) Bailey, M. F.; Dahl, L. F. *Inorg. Chem.* **1965**, *4*, 1140. (b) Bratton, W. K.; Cotton, F. A. *Inorg. Chem.* **1970**, *9*, 789. (c) Cotton, F. A.; Gage, L. D. *Nouv. J. Chim.* **1977**, *1*, 441. (d) Cotton, F. A.; Fanwick, P. E.; Gage, L. D. *J. Am. Chem. Soc.* **1980**, *102*, 1570. (e) Bürgi, H.-B.; Anderegg, G.; Bläuenstein, P. *Inorg. Chem.* **1981**, *20*, 3829. (f) Cotton, F. A.; Davison, A.; Day, V. W.; Fredrich, M. F.; Orvig, C.; Swanson, R. *Inorg. Chem.* **1982**, *21*, 1211. (g) Colmanet, S. F.; Mackay, M. *J. Chem. Soc., Chem. Commun.* **1987**, 705. (h) Anderegg, G.; Müller, E.; Zollinger, K. *Helv. Chim. Acta* **1983**, *66*, 1593. (i) Linder, K. E.; Dewan, J. C.; Davison, A. *Inorg. Chem.* **1989**, *28*, 3820.
(3) Cotton, F. A.; Daniels, L. *Inorg. Chem.* **1981**, *20*, 3051.
(4) Kryutchkov, S. V. *Dokl. Akad. Nauk. SSSR* **1986**, *288*, 389.
(5) Herrmann, W. A.; Alberto, R.; Kiprof, P.; Baumgärtner, F. *Angew. Chem.* **1990**, *102*, 208; *Angew. Chem., Int. Ed. Engl.* **1990**, *29*, 189.

0020-1669/91/1330-1086$02.50/0

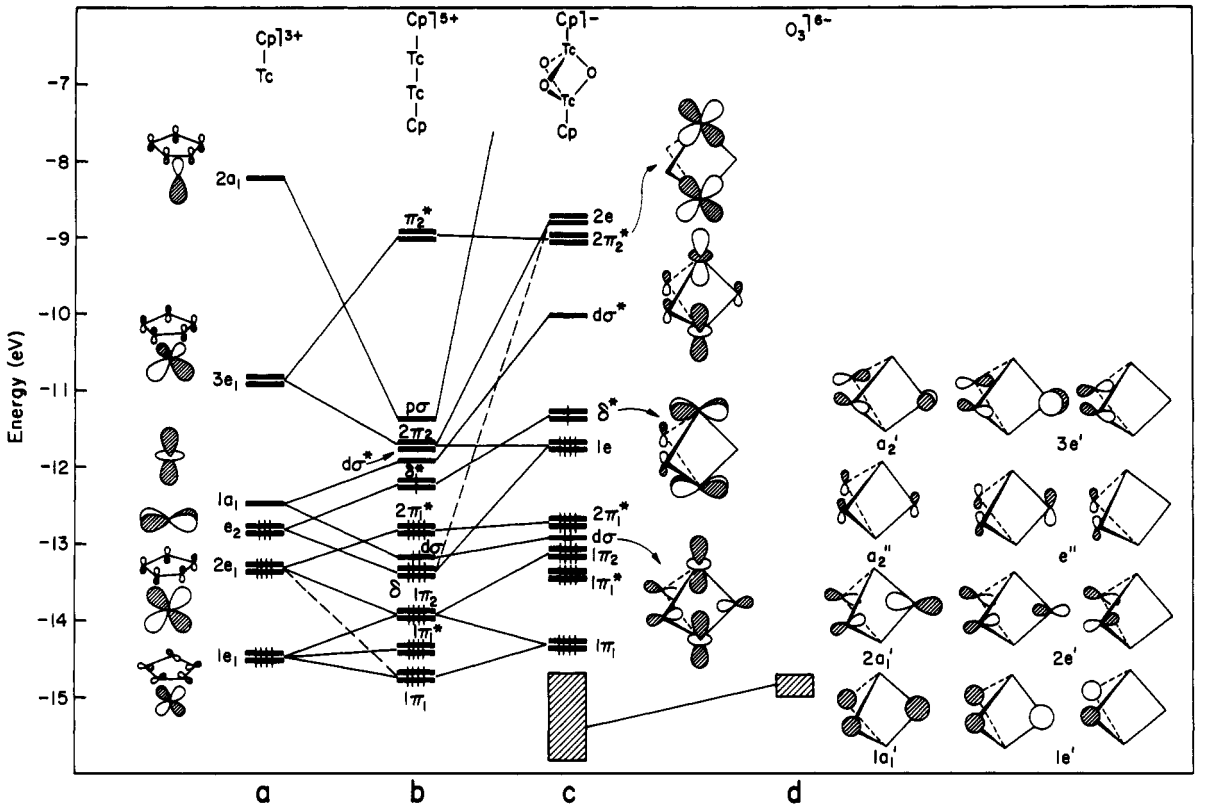

Figure 1. Molecular orbital interaction diagram of $CpTcO_3TcCp^-$: (a) orbitals of $CpTc^{3+}$; (b) two CpTc units brought together; (c) $Cp_2Tc_2O_3^-$ dimer; (d) orbitals of the bridging oxides.

starting point that we and others have found useful is to defocus from the distance and examine angular deformations from some archetypical structure.[6]

One can relate the polymer under consideration to a chain of face-sharing octahedra by a conceptual replacement of Cp by three bridging ligands. Were such a structure, **2**, formed simply by superimposing two perfect octahedra, the resulting angle at the bridging atom (here O), β, would be 70.5°, while the O–Tc–O angles (α) would be 90°.

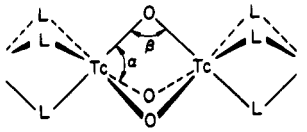

2

That is the reference geometry, no metal–metal interaction assumed. A way to gauge metal–metal bonding is by changes in β (and α); a significant decrease of β from 70.5° implies bonding, an increase, antibonding.[6] In the Tc polymer α is 97 and 96 (2)° and β is 59 and 61 (2)°. Consistent with the short metal–metal distance, one sees the attraction of the metals toward each other through the diminished β.

We have carried out a series of calculations to probe the reasons for this contraction and the very short Tc–Tc distance that goes with it. Several geometrical simplifications were made. The methyls of the C_5Me_5 ligands were replaced by hydrogens. The structure was symmetrized so that the Tc_2O_3 substructure was 3-fold symmetric, with Tc–O = 1.88 Å (in the observed structure there are two distances, 1.9 and 1.85 (2) Å) and α = 90°.

The extended Hückel[7] method is used to elucidate the bonding of this compound. Our approach is to study first a molecular model and then extend it to the solid state, where band structures, density of states (DOS), and crystal orbital overlap population (COOP) plots[8] will be examined. Also, by breaking down the system into some small building blocks (or fragments) and then allowing them to interact, we may gain a deeper understanding of the bonding. For further computational details, please refer to the Appendix.

Molecular Model

The unit cell of the polymer is $CpTcO_3Tc$. That is not a good molecular model, for it is unsymmetrical. The choice we make is that of $CpTcO_3TcCp^-$ (**3**), the charging chosen to force the same

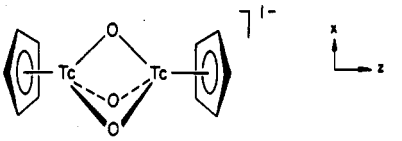

3

oxidation state of Tc in the model as in the polymer. There are several ways to build up this model. One could first construct CpTcTcCp from two CpTc units and then insert the three oxygens; alternatively one could cap a preformed TcO_3Tc by two Cp's. We will follow the first way.

First, let us look at the CpTc fragment with C_{5v} symmetry. Figure 1a displays its frontier orbitals. The $2e_1$ set is the result of bonding interaction between the Cp π orbitals, metal d_{xz} and d_{yz}. Its antibonding counterpart is the higher $3e_1$ set, with a second-order mixing from the metal p_x and p_y orbitals, which hybridize these metal-centered orbitals away from the Cp ligand. The e_2 set is composed mainly of metal d_{xy} and $d_{x^2-y^2}$, since these orbitals interact very weakly with the high-lying Cp e_2 π orbitals. $1a_1$ (d_{z^2}) is a nonbonding orbital. $2a_1$ is weakly bonding between Cp's a_1 orbital and metal s orbital but perturbed by the metal p_z

(6) Summerville, R. H.; Hoffmann, R. *J. Am. Chem. Soc.* **1979**, *101*, 3821.
(7) Hoffmann, R. *J. Chem. Phys.* **1963**, *39*, 1397. Hoffmann, R.; Lipscomb, W. N. *J. Chem. Phys.* **1962**, *36*, 2179; **1962**, *37*, 2872. Whangbo, M.-H.; Hoffmann, R. *J. Am. Chem. Soc.* **1978**, *100*, 6093.
(8) For a description of the methodology and the use of these indices in tracing down orbital interactions, see: Hoffmann, R. *Solids and Surfaces: A Chemist's View of Bonding in Extended Structures*; VCH: New York, 1988.

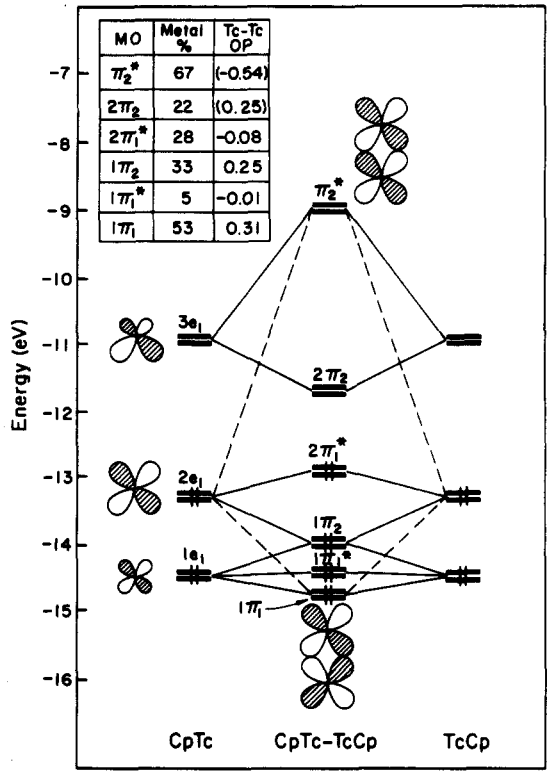

Figure 2. Complicated π-level interaction in $CpTcTcCp^{5+}$, with a table showing metal contribution and Tc–Tc OP for each MO. Numbers in parentheses denote a Tc–Tc OP if the orbital was occupied.

orbital. Only one set of the degenerate MO's is drawn in Figure 1. The CpTc orbitals are typical of an ML_3 fragment: e_2 and $1a_1$ are the "t_{2g}" set, $3e_1$ and $2a_1$ the hybrids pointing to vacant octahedral sites.[9]

Next we bring two of these fragments together and derive the MO's of CpTc–TcCp (D_{5h}) (Figure 1b). A note on symmetry: While D_{5h} is the correct point group at this stage, we will not use it to label the orbitals. This is because D_{5h} symmetry is lost when the three bridging oxygens are eventually inserted. The net symmetry at the end is relatively low, C_{2v}. However, it makes good sense to retain the pseudocylindrical symmetry that prevails, and so we will use σ, π, and δ labels. Also metal–Cp bonding orbitals will be subscripted as "1", and their antibonding orbitals "2", and metal–metal antibonding orbitals are labeled with an asterisk. Two e_2 sets form readily metal–metal δ-type orbitals. Interaction between two $1a_1$'s results in $d\sigma$ and $d\sigma^*$ orbitals. Similarly, $p\sigma$ is derived from $2a_1$ and is greatly stabilized.

The π-type interaction here is far more complicated. A six-orbital interaction takes place among the $1e_1$, $2e_1$, and $3e_1$ sets. Figure 2 isolates out this interaction. All the metal–metal bonding orbitals can mix with each other, and so can the metal–metal antibonding ones, since they have e′ and e″ symmetry, respectively, after interaction between the two fragments. The result is a very strongly metal–metal antibonding orbital, denoted π_2^*, at −9 eV, and a very strongly metal–metal bonding orbital, labeled $1\pi_1$, at −14.75 eV. The levels in the middle are primarily localized on the Cp rings. The table on Figure 2, which lists (1) the percentage contribution from the two Tc's and (2) Tc–Tc overlap population (OP) of each MO, supports this analysis. Note that $1\pi_2$, which contains only 33% metal character, contributes much of π-type metal–metal bonding. Later on, analogous effects will be seen clearly in the polymer.

The splitting of symmetry-related orbitals tells us how strongly the metals interact. These splittings are 1.5, 5.75, and 1.0 eV for σ, π, and δ bonding, respectively.[10] The contributions of the σ, π, and δ components to the Tc–Tc overlap population are listed in Table I.

Table I. Overlap Populations for Tc Dimers

	$[CpTcTcCp]^{5+}$	$[CpTc(\mu\text{-}O)_3TcCp]^-$
Tc–Tc	0.798	0.433
d_{z^2}–d_{z^2} (σ)	0.174	0.145
s–s (σ)	0.051	−0.010
d_{xz}–d_{xz} (π)	0.146	0.063
d_{yz}–d_{yz} (π)	0.146	0.063
$d_{x^2-y^2}$–$d_{x^2-y^2}$ (δ)	0.111	0.016
d_{xy}–d_{xy} (δ)	0.105	0.071

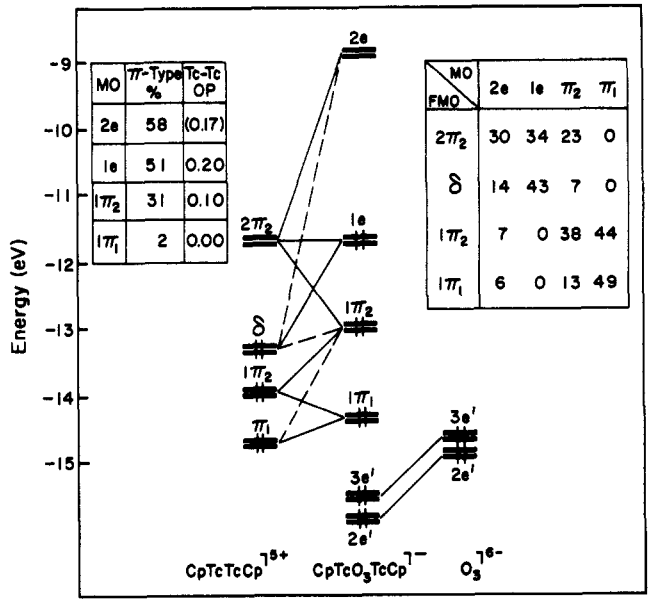

Figure 3. Molecular orbital diagram for π and δ mixing of $CpTcO_3TcCp^-$. Inset at the left shows the metal π-type contribution and its Tc–Tc OP for each MO; numbers in parentheses denote a Tc–Tc OP if the orbital was occupied. The right-hand inset gives the contribution of different FMO's to each MO, in percent.

Now the oxygens are brought in to interact with the above fragment to form $Tc_2(\mu\text{-}O)_3Cp_2$. The resulting MO's are in Figure 1c. The right-hand side of Figure 1 also shows the 12 2p orbitals of the $[O_3]^{6-}$ fragment, which has D_{3h} symmetry. Of the oxygen lone pairs, a_1' will interact with σ-type metal orbitals and a_2'' with σ^*; e′ will interact with π and δ type, while e″ will do so with π^* and δ^*. Symmetry prevents a_2' from mixing with any orbitals from the Tc fragment. The oxygen s orbitals, although at low energy, interact extensively with the metal $p\sigma$ orbital, which is strongly pushed up.

The symmetry of this model molecule is C_{2v}. This means that π and δ orbitals can mix. Nevertheless, we can usually identify the dominant orbital character, and we will apply the appropriate labels. The HOMO is located at −11.35 eV, with only one electron housed in the degenerate δ^* orbitals. Basically, π^* orbitals do not interact much with the oxygen fragment, due to poor overlap ($\langle\pi_2^*|e''\rangle = 0.02$). δ^*-type orbitals are pushed up, because of antibonding interaction with the oxygen e″ orbital ($\langle\delta^*|e''\rangle = 0.11$). $d\sigma$ and $d\sigma^*$ interact with $2a_1'$ and a_2'', respectively.

Metal-based π and δ orbitals, along with two more orbitals from the oxygen fragment, engage in a six-orbital interaction. Figure 3 shows the relevant (schematic) interaction diagram. The resulting MO's have both π and δ character. On the right side of Figure 3, the FMO composition of each MO is tabulated. The one labeled 2e actually has more π than δ, while in 1e the reverse is true. So, 2e, which comes mainly from $2\pi_2$, is now unfilled. It then contributes nothing to the Tc–Tc OP, resulting in a decrease in the overlap population (relative to CpTcTcCp), especially

(9) (a) Elian, M.; Chen, M. M. L.; Mingos, D. M. P.; Hoffmann, R. *Inorg. Chem.* **1976**, *15*, 1148. (b) Lauher, J. W.; Elian, M.; Summerville, R. H.; Hoffmann, R. *J. Am. Chem. Soc.* **1976**, *98*, 3219.

(10) The π splitting is complicated, as discussed above. We measured it by the $1\pi_1$, π_2^* energy difference; these orbitals have the most metal character.

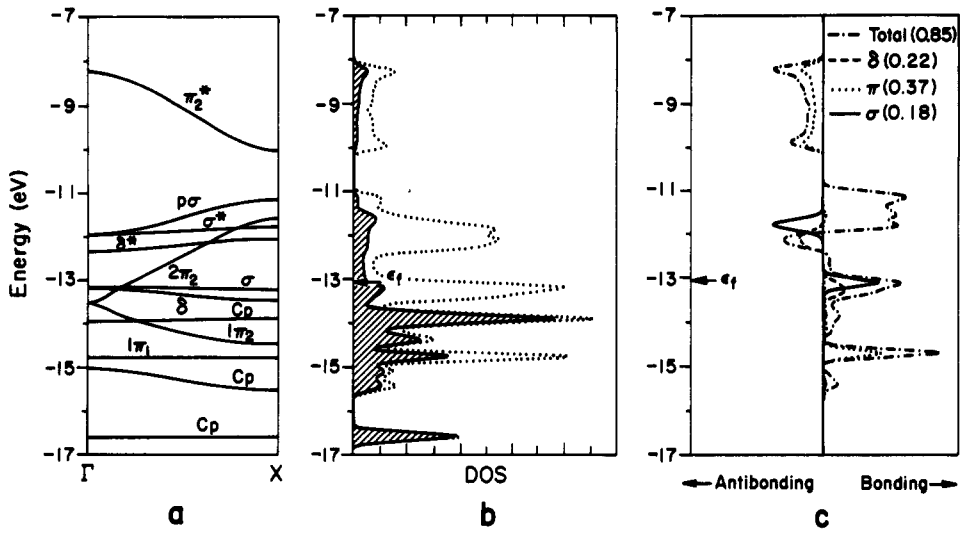

Figure 4. Band structure (a), density of states with a Cp projection (b), and Tc–Tc COOP curves (c) for Tc chain $[CpTc_2]_n^{6+}$.

in the π-type OP (See Table I). The decrease of the δ-type Tc–Tc overlap population follows from the same argument.

While this construction has taken some effort, we are now in a position to identify the orbitals responsible for metal–metal bonding. **4** shows the most important ones. Next to each MO

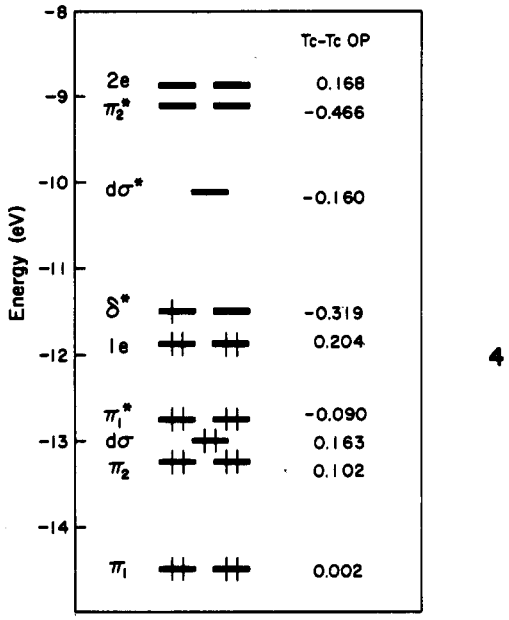

4

is listed its contribution to the metal–metal overlap population if it were fully occupied (by 2 or 4 electrons, as the case may be). All the levels below these valence ones contribute a total of 0.125 to the Tc–Tc OP.

Most of the metal–metal bonding among the occupied orbitals is concentrated in σ, 1e (π, δ), and δ^*. There is some π interaction also in π_1^* and π_2, but these just about cancel each other. While it is difficult to list this bond as $\sigma^2\pi^4\delta^*$ or $\sigma^2\delta^4\delta^*$ because of the extensive π, δ mixing in 1e, nevertheless it is clear that for an electron count of 7 the "bond order" is more like 2.5 than 3.5. An antibonding orbital is occupied by the last electron.

Building Up the Polymer: TcTcCp Subunit

The approach to the extended system will follow the molecular model study. Also, the notation of the crystal orbitals will be similar to the molecular case. Since the unit cell of the polymer is $CpTcO_3Tc$, we will start with a subunit, CpTcTc, and then interact it with three oxygens. The geometry is idealized from that of the real polymer, Tc–Tc taken as 1.87 Å. In order to keep the same oxidation state on each atom, the calculations are all done on $[Tc\text{–}Tc\text{–}Cp]^{6+}$ (we will call this the Tc chain hereafter). This chain has D_{5h} symmetry in real space, with a C_5 axis along the Tc–Tc bond. However, in reciprocal space there is only C_{5v} symmetry along the reciprocal vector, k_z, except at the zone center (Γ, $k_z = 0$) and zone boundary (X, $k_z = 0.5$) where the extra mirror plane, σ_{xy}, raises the point symmetry to D_{5h}. Figure 4 shows the band structure, the total DOS with a Cp projection, and the Tc–Tc COOP curves decomposed into $d\sigma$ (d_{z^2}–d_{z^2}), π (d_{xz}–d_{xz}, d_{yz}–d_{yz}), and δ ($d_{x^2-y^2}$–$d_{x^2-y^2}$, d_{xy}–d_{xy}) contributions.

Let us construct the band structure of the $[Tc\text{–}Tc\text{–}Cp]^{6+}$ unit in Figure 4a. Note that the Tc_2 units are far away from each other in the polymer. Thus, those orbitals that are primarily metal-based will interact (acquire bandwidth) only through their mixing with the cyclopentadienyl ligand. The bandwidth is a clue as to how much Cp and the metals interact. The π-type bands have greater bandwidth because they interact most with the Cp π orbitals, as we discussed in the molecular analysis, while σ- and δ-type bands are quite flat because they remain essentially nonbonding with respect to Cp, localized on Tc_2. Since this Tc chain has C_{5v} symmetry along the symmetry line ΓX, the bands labeled $\sigma(\sigma^*)$ have $a_1(a_2)$ symmetry; π has e_1 and δ has e_2 symmetry.

Now what controls the way the bands run?[8] Cp π orbitals are always antisymmetric between two unit cells. Thus, they can only mix in with the antisymmetric combination of the metal–metal fragment between two unit cells. So, symmetry prevents some mixing of Cp π orbitals with the Tc orbitals. For example, $p\sigma$ runs up in energy from Γ to X because Cp π orbitals can mix in at the zone boundary only, thus lowering the energy of this point (see **5a**). Take δ^* as another example. This time, Cp π orbitals

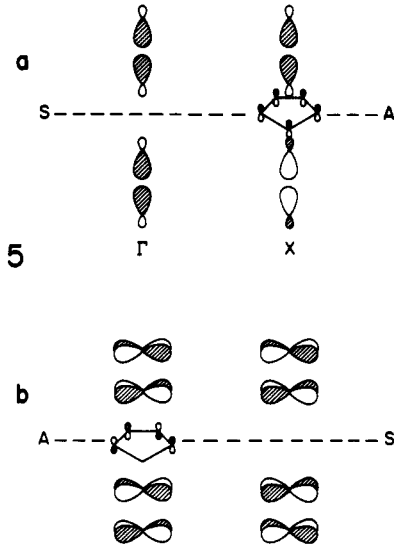

5

can mix in at X but not Γ (**5b**). So, by coupling with the Cp π

Table II. Calculated Indices for Tc Dimers and Polymers

	$[Tc-Tc-Cp]_n^{6+}$	$[Tc(\mu\text{-}O)_3TcCp]_n$	$[Tc_2Cl_8]^{2-}$	$Tc_2(\mu\text{-}O)_2(H_2EDTA)_2$	$Tc_2(CO)_{10}$
Tc–Tc, Å	1.87	1.87	2.14	2.33	3.04
			Overlap Populations		
Tc–Tc	0.846	0.408	0.870	0.292	0.252
d_{z^2}–d_{z^2} (σ)	0.175	0.149	0.144	0.129	0.037
s–s (σ)	0.047	0.000	0.020	0.003	0.008
d_{xz}–d_{xz} (π)	0.187	0.089	0.196	−0.006	−0.003
d_{yz}–d_{yz} (π)	0.187	0.089	0.196	0.167	−0.003
$d_{x^2-y^2}$–$d_{x^2-y^2}$ (δ)	0.110	0.016	0.000	0.004	0
d_{xy}–d_{xy} (δ)	0.110	0.016	0.060	−0.039	0
Tc–O		0.340		0.389	

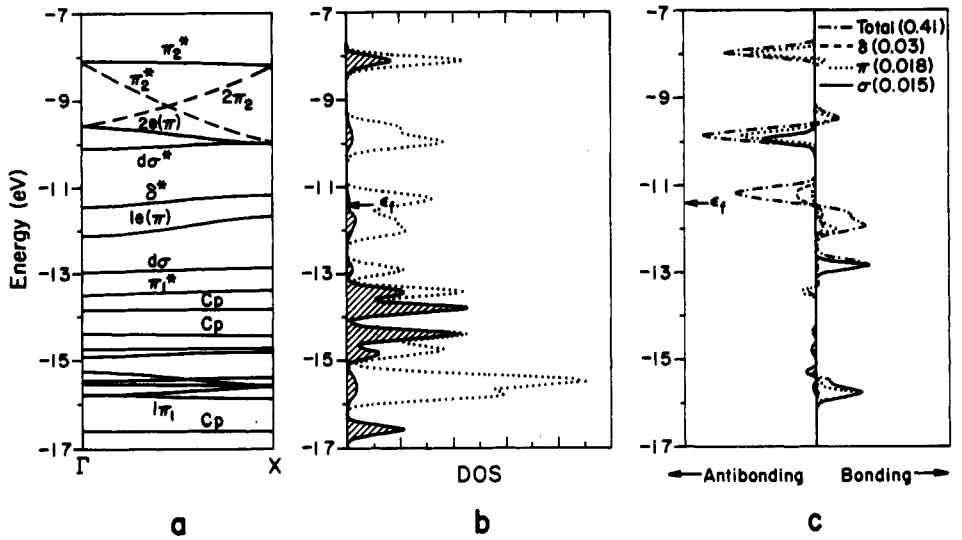

Figure 5. Band structure (a), density of states with a Cp projection (b), and Tc–Tc COOP curves (c) for Tc polymer $[CpTcO_3Tc]_n$.

orbitals, one end of each band can be stabiized along k_z.

The shape of the π-type bands is easy to understand. Since only Cp π orbitals are involved, we could think of a Cp ring as a pseudo Tc atom. What we are dealing with then is just a linear chain with a tripled unit cell. The band gets folded three times,[8] as shown in **6**.

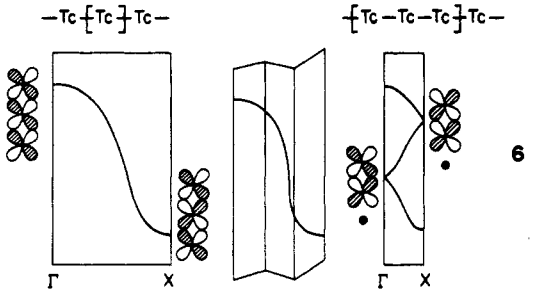

6

The σ, π, and δ contributions split cleanly into bonding and antibonding peaks (Figure 4c). The energy splittings read from Figure 4c between σ/σ^*, π/π^*, and δ/δ^* are 1.3, 5.5, and 1.0 eV, respectively, values close to those in the molecular model. Table II also lists other computed indices of bonding.

The σ and δ peaks are located around −13 and −13.4 eV, while σ^* and δ^* are near −12 eV. Since π-type orbitals interact most with Cp, they show up across a wide range of DOS, −15.5 to −11.5 eV. The π contribution to the COOP shows a broad flat region between −11.5 and −14.5 eV. The explanation follows from the molecular study; there is a complicated higher order mixing of π-type orbitals. The very big peak around −11 to −12 eV on the COOP curves is contributed by the pσ ($s + p_z - s + p_z$) band. Later on, in the real polymer, this band will be greatly destabilized.

Electronic Structure of $[Tc(\mu\text{-}O)_3TcCp]_n$

For the composite polymer $[Tc(\mu\text{-}O)_3TcCp]_n$ (from here on, it will be called "the polymer"), the C_{5z} rotation axis disappears in real space, so the chain has only C_{2v} symmetry, with a C_{2x} rotation axis. Along k_z, only σ_{yz} remains. At the zone center and the zone boundary one also has σ_{xy} as a symmetry element. This means the bands will have either "a" or "b" symmetry. Therefore, π and δ can mix. The new band structure (Figure 5a) looks deceptively simple because of avoided crossings between the original π and δ bonds. However, the dashed lines show how the original bands actually correlate and would run if there were no avoided crossing. It should be noted that the bands only appear to be degenerate. For example, δ^* consists of two bands very close in energy to each other.

Compared to the CpTcTc chain of the previous structure, almost all the bands now have been pushed up. This is due to the fact that these bands are antibonding between the $[TcTcCp]^{6+}$ fragment and the appropriate orbitals from the oxygen fragment. We can verify this by looking at the Tc–O COOP curve (Figure 6).

Thus, dσ and dσ^* have both been pushed up, 0.30 (still below the Fermi level) and 1.88 eV, respectively. δ and δ^* are pushed up by 1.5 and 0.881 eV, respectively, relative to the analogous bands in the TcTcCp chain. Since some states of the π^* and δ^* bands are now filled (Figure 5), the Tc–Tc overlap population has decreased, as seen in the OP entry in Table II. Also, some σ^* character is incorporated into the Tc–O bonding levels, resulting in a slight decrease of d_{z^2}–d_{z^2} OP.

The pσ band has been greatly destabilized because it interacts with the lowest lying oxygen $1a_1'$ orbital, which is, on the other hand, stabilized. The overlap ⟨metal pσ|oxygen $1a_1'$⟩ is 0.534.

Low-lying oxygen-centered states account for most of the Tc–O overlap population. Thus, if electrons are filled to −14 eV, then the Tc–O OP is 0.505. Filling electrons up to the Fermi energy, which is now at −11.4 eV, results in a total Tc–O OP of 0.345. The metal block orbitals below the Fermi level are thus actually Tc–O antibonding.

π_2^* remains in the same energy region, since its energy match with oxygen e″ is poor, as in the molecular case. From our previous analysis, the π^* orbital does not interact much with the oxygens; this still holds in the polymer. The four bands labeled 1e and 2e are a mixture of π and δ, with more π character in 2e

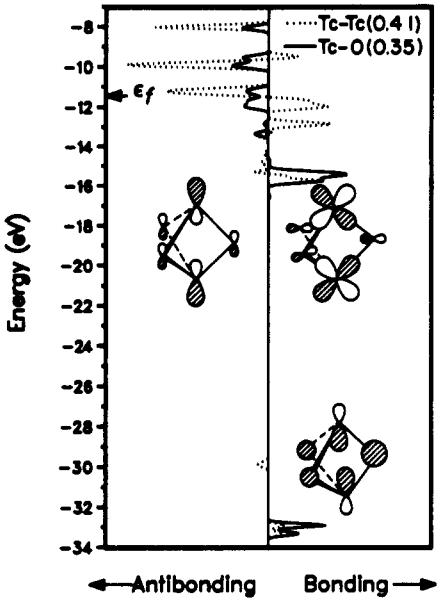

Figure 6. Tc–O and Tc–Tc COOP curves for the Tc polymer.

and more δ in 1e. The 1e, 2e notation is used here to make a correspondence to the molecular model. The original $2\pi_2$ and δ band interact with 2e″ and 3e″ of $(O_3)^{6-}$ and are pushed up. The exception is the π_1 band, which was originally at −15 eV and now at −16 eV. This is the result of mixing between all the π-type orbitals. Since most of the π states are pushed up above the Fermi energy, the π OP has decreased. Moreover, part of the original δ bands are pushed up. In addition, filling up some δ^* bands makes the δ OP decrease from 0.22 to 0.07.

We have also partitioned the Tc–Tc overlap population on an atomic orbital (AO) basis in Table II. There is a 36% contribution from $d\sigma$, 44% from π, and 17.4% from δ. The σ OP of the polymer has decreased a little, 15%, compared to that of the TcTcCp chain. However, the π and the δ OP have decreased a lot, 52% for π and 68% for δ. The overlaps $\langle d_{xz}|d_{xz}\rangle$ and $\langle d_{yz}|d_{yz}\rangle$ are 0.174 before and after the interaction, since they depend mainly on the distance between the two atoms. However, the overlap population is a sum, $OP_{ij} = 2\sum nc_ic_jS_{ij}$, up to the Fermi level, where n is the electron occupation number. Thus, the π-bonding overlap stays the same, except that some π states are pushed up above the Fermi level, decreasing the overlap populations. This is also true for metal δ-type orbitals.

After all the above factors are added up, the Tc–Tc overlap population has decreased to 0.408. There is one electron in δ^* (two almost-degenerate bands). If this electron is removed, then both the Tc–Tc and Tc–O bonds should strengthen. Oxidizing this polymer may do the trick. A calculation with one less electron has been carried out, with the result that the Tc–Tc and Tc–O OP's become 0.482 and 0.357, respectively.

A possibility to be considered for this polymer is a pseudo-first-order Peierls distortion. Since we have one electron per two bands, then if there is a distortion every four unit cells, electrons miight pair up to form a low-spin state. This is shown schematically in **7**. An alternative is a high-spin polymer, **8**. The

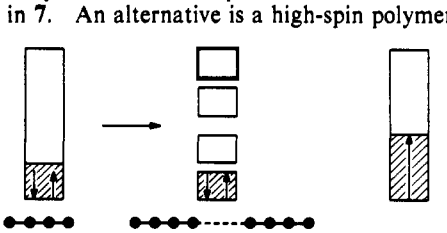

7 **8**

experimental data show no sign of a distortion increasing the unit cell. The polymer is reported as being slightly magnetic, yet a reasonable NMR spectrum is obtained.[1] So the magnetic properties of the $CpTc_2O_3$ chain remain a puzzle.

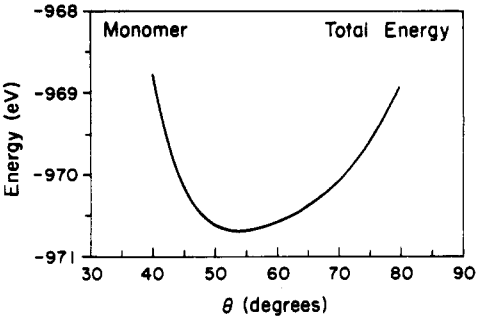

Figure 7. Energy vs θ for a $CpTcO_3^{3.5+}$ monomer.

Geometrical Preference

Now that we have discussed the electronic structure of this compound, we are left with the question, why does it prefer this geometry, with Tc–Tc unusually short at 1.87 Å and β at around 60°? One idea is to seek the geometrical preference within a "monomer", $CpTcO_3^{3.5-}$ (**9**). θ is defined as the angle between

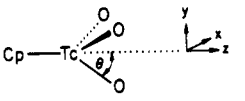

9

the z axis and a Tc–O bond. We allow this monomer to distort, to see what is its optimum θ. The energy curve computed and illustrated in Figure 7 has a minimum at 55°, close to the angle of a regular octahedron. Were the compound to "dimerize" to $CpTcO_3TcCp$, the angle Tc–O–Tc, β, should be the complement of 2θ, which is 70°. As mentioned before, a decrease in β implies bonding between the two metals. And that is what happens. So the source of the contraction is to be found in the dimer, not in the geometric preferences of the monomer.

Let us take another tack: Three oxygen atoms are allowed to approach the Tc fragment in the Tc polymer. The total energy and several overlap populations are monitored at the same time. In this case, the Tc–Tc bond length is fixed at 1.87 Å and the distance of Tc to the plane of the Cp ring is taken as 2.06 Å. But the Tc–O bond length varies as the oxygens approach. So, when the oxygens are far from Tc, Tc–O is long and β is small, while when Tc–O is short, β is large. A picture at the top of Figure 8 shows this movement. Figure 8 plots energy and overlap populations (Tc–Tc and Tc–O) vs β. The total energy curve has a minimum around 60°, which is the experimental finding. The Tc–Tc OP decreases with β, while the Tc–O OP increases with it.

β cannot be too small, because there will be no Tc–O bonding. If the Tc–O distance is increased, the 2e (π) bands will be less pushed up, thus filling up more π-bonding states instead of δ^*. This strengthens the Tc–Tc overlap population. There are then two constraints that govern the system: optimizatioin of both the Tc–Tc and Tc–O bond strengths.

Next we constructed a Walsh diagram in Figure 9, plotting the energies of different bands at either Γ or X, as a function of β. A minimum at $\beta = 60°$ is found from the Walsh diagram at the Γ and X points.

In general it is not easy to draw Walsh diagrams for solids, because of the way bands vary with k. However, it is reasonably safe to do this here, because all the bands are roughly parallel to each other. So plotting the energy at Γ or X will represent the trend of these bands across the Brillouin zone. A further complication, however, is that there is an avoided band crossing, near $\beta = 65°$. This is responsible for the discontinuities in the overlap populations. When β is bigger than 65°, δ^* even comes below 1e (δ), since the Tc–O distance is so small that δ and 2e′, 3e′ have a big interaction.

Since there is a sharp minimum in energy of all the bands at 60°, we suspected that there may be another reason for this special

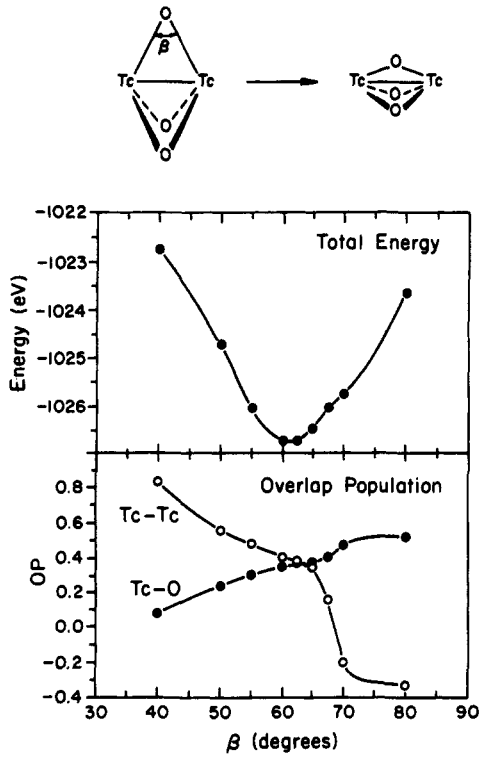

Figure 8. Energy and Tc–Tc and Tc–O OP vs β. The Tc–Tc distance is kept as a constant. Note the discontinuity near $\beta = 65°$, due to a level crossing.

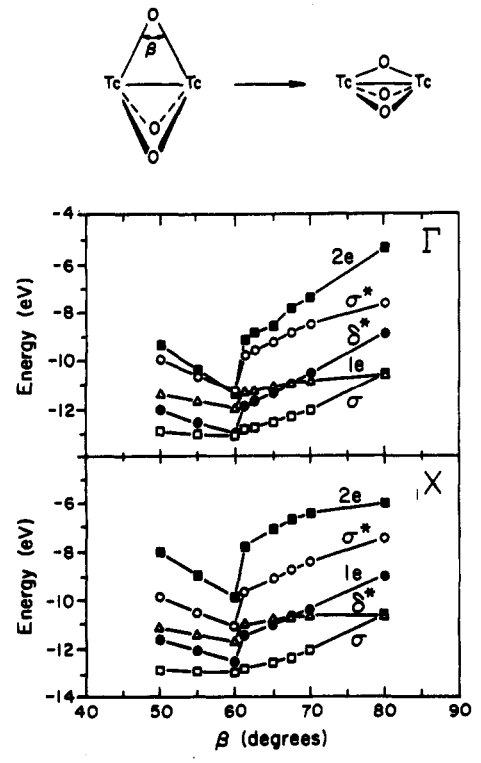

Figure 9. Walsh diagrams for the polymer, varying β. There is a discontinuity near $\beta = 65°$, due to a level crossing.

geometrical preference. Around the Fermi energy, the bands are all Tc–O antibonding (Figure 6). In order to minimize this antibonding, the maximum electron density of the O_3 fragment should be near or on the nodal plane of the metal fragment. When β increases, the electron density of the ligands begins to approach the nodal plane of the appropriate metal fragment orbitals, thus minimizing the antibonding effect. It reaches a minimum at around $\beta = 60°$. For example, the Tc–O OP between metal's d_{z^2} and oxygen's p_x changes from bonding to antibonding as a function of β. At 55° it reaches zero. This corresponds to an overlap, $\langle d_{z^2}|p_x\rangle$, of 0.002 at 55°. In another example, the OP between Tc d_{xy} and oxygen p_y changes from antibonding to bonding with respect to β and reaches zero at 60° (the corresponding overlap is 0.008 at that angle). Of course, different crystal orbitals will have different nodal planes, so the local minimum at 60° represents some average of all the interactions.

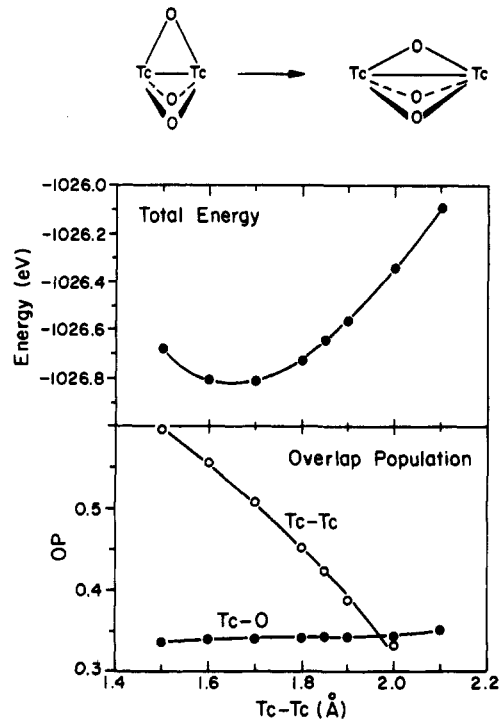

Figure 10. Energy and Tc–Tc and Tc–O OP vs Tc–Tc distance when Tc–O distance is kept as a constant.

Table III. Extended Hückel Parameters

atom	orbital	H_{ii}, eV	ζ_1	ζ_2	c_1[a]	c_2[a]
Tc	5s	−10.07	2.020			
	5p	−5.40	1.980			
	4d	−12.82	4.900	2.094	0.5715	0.6012
O	2s	−32.30	2.275			
	2p	−14.80	2.275			
C	2s	−21.40	1.625			
	2p	−11.40	1.625			
H	1s	−13.60	1.300			

[a] Coefficients used in the double-ζ expansion of the d orbitals.

In still another approach to the problem, we varied the metal–metal distance in the polymer, while keeping Tc–O and Tc–Cp constant. The results are shown in Figure 10. The minimum of the total energy curve is around 1.7 Å. The experimental distance is 1.867 Å. The calculated separation is not too bad, given the general unreliability of the extended Hückel method for distances.

Tc–Tc Bond in the Polymer

What is the multiplicity of the Tc–Tc bond in this polymer? The traditional way of figuring the bond order of a metal dimer is to count the filled bonding levels that are metal-based and to subtract the filled antibonding ones. It was not easy to do so in the molecular model $CpTcO_3TcCp^-$; it is still more difficult to do so in the polymer. We have to try other approaches to this question.

The compound $Tc_2Cl_8^{2-}$ is known to have a quadruple bond, while $Tc_2(CO)_{10}$[2a] has a bond order of 1. Note that the OP value of our compound falls between these two. We have listed in Table II their AO by AO Tc–Tc overlap populations for comparison. The d_{z^2}–d_{z^2} and δ-type overlap populations are similar in the Tc polymer and $Tc_2Cl_8^{2-}$, which suggests that in our compound the

σ and δ metal bonding are comparable to that in the $Tc_2Cl_8^{2-}$ compound. However, the Tc polymer has a much smaller π-overlap population, because, as we analyzed above, some π orbitals are used for interaction with the oxygens.

The compound $Tc_2(\mu\text{-}O)_2(H_2EDTA)_2^{2e}$ (**10**) was suggested to have a long triple metal–metal bond, with a configuration of $\sigma^2\pi^2\delta^{*2}$. But its Tc–Tc overlap population is only 0.292, calculated

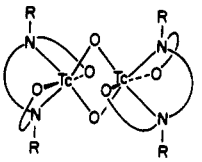

10

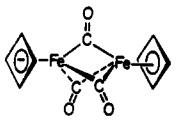

11

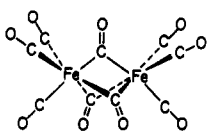

12

by the extended Hückel method. Another interesting relevant compound is tris(μ-carbonyl)bis(1,2-diphenyl-3,4-di-*tert*-butylcyclobutadiene)diiron (**11**). Our group has done calculations on **11** in the past and suggested that it may have a multiple Fe–Fe bond.[6] The 18-electron rule would assign it a triple bond, and the Fe–Fe distance indeed is short, 2.18 Å. However, the Fe–Fe overlap population is only 0.165. Also, $Fe_2(CO)_9$ (**12**) has a single bond, even though the Fe–Fe overlap population in an extended Hückel calculation is −0.001.[11] So overlap populations by themselves do not always correlate with common preconceptions on the number of bonds.

In general there are problems with describing the extent of metal–metal bonding in bridged or supported systems. We actually believe that the bond in Tc_2O_3Cp *is* very short not because it is extraordinarily strong but because it operates "on top" of a constrained short contact of the metals imposed by the bridges. Consider the simple triply bridged system, dimer or polymer, **13**.

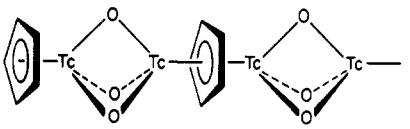

13

At β = 70° and Tc–O = 1.88 Å, the Tc–Tc distance would be 2.16 Å, *in the absence of any Tc–Tc bonding*. A Tc–Tc bond of multiplicity around 2.5 (that is what we conclude from the model dimer) shortens Tc–Tc to 1.87 Å. We do not think this is unreasonable, given that a quadruple bond is 0.9 Å shorter for Tc than a single bond, with no bridging.

Acknowledgment. A.W.E.C. wishes to thank Pere Alemany and Yat-Ting Wong for helpful discussions. We are grateful to Jane Jorgensen and Elisabeth Fields for their drawings. This work was supported by the Cooperative Research Grant in Basic Science, CCB86/4004/88, from the U.S.-Spanish Joint Committee for Scientific and Technological Cooperation.

Appendix

All calculations are carried out by the tight-binding extended Hückel method.[7] Table III lists the atomic parameters used. A set of 20 k points were used.

(11) Mealli, C.; Proserpio, D. M. *J. Organomet. Chem.* **1990**, *386*, 203.

Contribution from the Isotope and Structural Chemistry Group (INC-4), Los Alamos National Laboratory, Los Alamos, New Mexico 87545

Time-Resolved Resonance Raman Study of the $\delta\delta^*$ Excited State of $Re_2Cl_8^{2-}$ and $Re_2Br_8^{2-}$

Jon R. Schoonover, Richard F. Dallinger,[1] Patrick M. Killough, Alfred P. Sattelberger, and William H. Woodruff*

Received July 3, 1990

Time-resolved resonance Raman (TR^3) spectra have been obtained for $Re_2X_8^{2-}$ (X = Cl, Br) in the $^1A_{2u}$ ($\delta\delta^*$) electronically excited state, at ambient temperature in solution. The TR^3 spectra exhibit Raman peaks that are assigned to the three symmetric vibrations of the excited state: the Re–Re stretch, Re–X stretch, and the Re–Re–X deformation. In addition, a depolarized peak attributed to an asymmetric X–Re–X bend is observed. Comparison of the TR^3 results to single-crystal vibronic spectra reported by others clearly shows the effects of crystal constraints and observation time scale upon the structure of the $\delta\delta^*$ excited state. The excited-state metal–metal bond distance is inferred to be 0.03–0.04 Å shorter in solution than in the crystal. The TR^3 data, obtained in solution on the nanosecond time scale, indicate that the excited state relaxes to a staggered molecular structure (D_4 or D_{4d} symmetry). The vibronic data, obtained on single crystals under cryogenic conditions, are consistent with an eclipsed (D_{4h}) structure, similar to that of the ground state. A comparative TR^3 study of quadruply bonded complexes, including both octahalodirhenate ions and $Mo_2(PMe_3)_4Cl_4$ (which is precluded by steric factors from significant torsional distortion about the metal–metal bond), was essential in elucidating the excited-state structures.

Introduction

Time-resolved resonance Raman (TR^3) spectroscopy allows direct observation of the molecular vibrations of short-lived chemical species. An important application of TR^3 spectroscopy is in the determination of vibrational spectra of molecules in electronically excited states under ambient conditions (room temperature, fluid solution).[2,3] Previous experimental approaches to determining structural features of the electronically excited states of relatively complex molecules have been confined primarily to Franck–Condon analysis of the resolved vibronic spectra. This approach generally requires the absorption spectrum to be recorded

(1) Permanent address: Chemistry Department, Wabash College, Crawfordsville, IN.

(2) Dallinger, R. F.; Farquharson, S.; Woodruff, W. H.; Rodgers, M. A. J. *J. Am. Chem. Soc.* **1981**, *103*, 7434.

(3) Bradley, P. G.; Kress, N.; Hornberger, B. A.; Dallinger, R. F.; Woodruff, W. H. *J. Am. Chem. Soc.* **1981**, *103*, 7441.

0020-1669/91/1330-1093$02.50/0